Antibiofilm Efficiency of CaF_2/TiO_2 Strontium Borate Bioactive Glass Composites against *Pseudomonas aeruginosa* and Gamma Radiation Effect

Eman Mohamed Abou Hussein[1], Noha Mohamed Abou Hussien[2], Sabrin Ragab Mohamed Ibrahim[3,4*], Mahmoud Abdelkhalek Elfaky[5,6], and Tamer Dawod Abdelaziz[3]

[1]*Radiation Chemistry Department, National Center for Radiation Research and Technology, Atomic Energy Authority, P.O. Box 8029, Nasr City, Cairo 11371, Egypt*

[2]*Department of Medical Parasitology, Faculty of Medicine, Menoufia University, Shebin El-Kom, Menoufia 13829, Egypt*

[3]*Department of Chemistry, Preparatory Year Program, Batterjee Medical College, Jeddah 21442, Saudi Arabia*

[4]*Department of Pharmacognosy, Faculty of Pharmacy, Assiut University, Assiut 71526, Egypt*

[5]*Center for Artificial Intelligence in Precision Medicines, King Abdulaziz University, Jeddah 21589, Saudi Arabia*

[6]*Department of Natural Products and Alternative Medicine, Faculty of Pharmacy, King Abdulaziz University, Jeddah 21589, Saudi Arabia*

* ***Corresponding author:***

email: sabrin.ibrahim@bmc.edu.sa

Received: May 14, 2023
Accepted: October 27, 2023

DOI: 10.22146/ijc.84412

Abstract: *Microbial drug resistance has emerged as one of the most fundamental health threats. The current work aims to assess the antibacterial and antibiofilm potential of strontium borate bio-glasses (BBGs). Three CaF_2/TiO_2 strontium borate compositions have been prepared through melting annealing methods. The XRD pattern displays the amorphous nature of the glassy samples. The primary structural components of the borate, the trigonal BO_3 and tetrahedral BO_4 group, can be observed in FTIR spectra. Sharpness and shifting peaks to longer wavenumbers were evident after 40 kGy of gamma radiation. In contrast, density and molar volume (V_m) reveal an obvious change after irradiation. The agar diffusion technique was conducted as a preliminary screening of the antibacterial activity against* Pseudomonas aeruginosa*. The studied samples possessed no antimicrobial activity toward this strain; however, samples with 2% CaF_2 strontium borate (T1) and 5% TiO_2 strontium borate (T3) had higher biofilm inhibition potential (inhibition percentages of 75.17 and 65.77%, respectively). The gamma irradiation procedure had an unexpected detrimental effect on the bio-glass antibiofilm activity, making it unsuitable for use in sterilization procedures. Collectively, BBGs could be further investigated as possible antibacterial agents against biofilm-producing resistant strains.*

Keywords: *borate bioglass; FTIR; antibacterial;* Pseudomonas aeruginosa*; biofilm inhibition*

■ INTRODUCTION

Infectious diseases represent the second-leading cause of human deaths worldwide [1]. Human microbial infections can be caused by both extrinsic and intrinsic factors [2]. The use of antibiotics to inhibit the growth of germs is a common strategy. However, excessive and unwarranted usage of antibiotics leads to the development of antimicrobial resistance (AMR). AMR has become one of the most outstanding public health concerns, and the prevalence of bacterial resistance keeps increasing [3]. AMR is predicted to be responsible for 4.95 million fatalities in 2019, of which 1.27 million are attributable to bacterial resistance. Australasia had the lowest rate (6.5/100,000) while western sub-Saharan Africa had the highest (27.3/100,000) [1]. Additionally, high antibiotic dosages can also have undesirable side effects and severe toxicity [4]. Besides, many antibiotics

have lost their efficacy after overuse and long-term misuse, generating an emergency status [3].

Bioactive glasses (BGs) are a class of biocompatible materials that can be utilized to eliminate the dangers and risks associated with metal or plastic surgery implants [5], as well as to boost the regeneration of bone joints and bone surgeries [6]. Due to the antibacterial potential of several BGs formulations, they are ideal for use in bone-regenerating surgical operations that are accompanied by a significant risk of infection, such as oral bone and osteomyelitis defects [7]. Additionally, BGs were reported to be an effective treatment for osteomyelitis due to their potential against most of the bacteria that cause osteomyelitis and their osteo-stimulatory and osteoconductive capabilities [8-9]. Numerous researchers have examined several metal ions (Ag^{+}, Cu^{2+}, and Zn^{2+}) for their potential application as antibacterial agents against bacteria and fungi [10-11]. Drago et al. [8] reported that "needle-like" sharp glass shards punctured or dented the bacterial cell wall, allowing antimicrobial chemicals to penetrate the cytoplasm. Also, recent investigations have shown that BGs have strong anti-biofilm action in a variety of formulations. Ag^{+}, Cu^{+}, Cu^{2+}, Ga^{3+}, Ti^{4+}, and Zn^{2+} are a few examples of ions that can be used in doped BG to target the suppression and rupture of bacterial biofilms [12-15]. BGs include silicate bioglasses (SBGs) and borate bioglasses (BBGs) types. In comparison to SBGs, BBGs have several benefits, including faster healing rates for wounds than silicate-based glasses [16]. Numerous studies have recently focused on osteointegration or antimicrobial metal oxides in different borate glass compositions [17]. A recent study showed that the inflammatory response of the cells can be modulated by the inclusion of boron in BGs [18]. A lot of non-bridging oxygens (NBOs) are created when there is a high modifier concentration, which disrupts the borate network's connection. Due to this disruption, the produced borate glasses are extremely vulnerable to chemical deterioration, and the corrosion process can be accelerated due to the increase of NBOs [19].

Pseudomonas aeruginosa is among the six bacterial pathogens that are usually associated with AMR [20]. This bacterium causes chronic lung infections in people with cystic fibrosis and chronic obstructive pulmonary disease, ventilator-associated pneumonia in people who have been intubated, and chronic infections of the urinary system in people who have permanent bladder catheters. It is also well-known for being a significant chronic infection source due to its capacity to form biofilms, which are aggregations of bacteria with an extracellular matrix that are resistant to antibiotic therapy [21]. These biofilm infections are difficult to be eradicated with antibiotics [22].

The process of effectively destroying or decreasing practically all microorganisms is referred to as sterilization. Numerous sterilizing techniques are available, including gamma radiation, heat, pressurized steam, formaldehyde, peracetic acid, dry ethylene oxide, gas plasma, and heat. The selection of a sterilizing technique is mostly influenced by non-hazardous tools and materials [23]. This study focused on preparing and characterizing metallic element-doped BBGs and assessing their antibacterial capacity against *P. aeruginosa*. This study investigated the impact of gamma radiation and different metal oxides on the antibacterial activity of these BBGs to identify their superior performance in medical and surgical applications.

■ EXPERIMENTAL SECTION

Materials

The materials used in this study were H_3BO_3, $SrCO_3$, Li_2CO_3, Na_2CO_3, TiO_2, and CaF_2 (purity 99.9%) purchased from Sigma Aldrich. Ethanol (99.9% purity, Sigma-Aldrich), sodium acetate (99.9% purity, Sigma-Aldrich), phosphate-buffered saline (PBS, Sigma-Aldrich), Muller-Hinton agar (HiMedia), Muller-Hinton broth (HiMedia), ciprofloxacin HCl (Sigma-Aldrich), and crystal violet (Sigma-Aldrich) were used in this work.

Instrumentation

The instrumentations utilized for the characterization of the BBGs were X-ray diffraction (XRD, Shimadzu-Japan), XRF Philips sequential X-ray spectrometer-2400, and FTIR spectrophotometer (VERTEX 70, FT/IR-430, Shimadzu-Japan). ^{60}Co

gamma cell (2000 Ci) was used for gamma irradiation at EAEA, with a dosage rate of 0.717 kGy/h and at a temperature of 30 °C. A UV-visible spectrophotometer (Labomed Inc., USA) was used for measuring optical density.

Procedure

Glass preparation and characterization

By using the typical melting-annealing method, three BBG samples were prepared. Glasses were made using H_3BO_3, $SrCO_3$, Li_2CO_3, Na_2CO_3, TiO_2, and CaF_2, whose calculated compositions are shown in Table 1.

Three batches that were precisely weighed were melted for 2 h at 850 °C in a muffle furnace with frequent, careful stirring to produce more homogeneous melts. The melts were then quickly transferred to warmed stainless-steel molds and annealed at 350 °C to remove any tension or thermal strain residues from the prepared glasses. Previously, the annealing muffle was turned off after 1 h to allow the glass samples to cool inside of it at a pace of 30 °C/h until room temperature. Fine powder glass samples have been prepared to examine the glass properties.

The employed technique used to examine the presence or absence of crystalline structure in glass is the XRD technique at a scanning rate of 8°/min and 2θ from 4° to 90°. XRF analysis was used to determine the chemical composition of the BBG samples. FTIR spectrophotometer operating in the 400–4000 cm^{-1} wavenumber range.

Using Archimedes' equation, the density of the examined glasses was calculated (Eq. (1)).

$$\rho = \frac{a}{(a-b)} \times 0.86 \quad (1)$$

In this formula, ρ is the density of the glass sample, a is the weight of the glass sample in air, b is its weight in xylene, and 0.86 is the density of xylene at 20 °C. According to Chanshetti et al. [24] calculations, the molar volume (V_m) was determined. Glasses were exposed to 40 kGy of gamma radiation.

Table 1. Lists the ingredients in the prepared BBG samples

Composition mol.% /Bioactive glass	B_2O_3	SrO	Li_2O	Na_2O	TiO_2	CaF_2
T1	50	25	15	5	0	2
T2	50	28	15	5	2	0
T3	50	28	15	5	5	0

Antibacterial evaluation

The antibacterial potential of the BBG samples was assessed against a quality control isolate of *P. aeruginosa* ATCC-27853 (Microbiology Lab, KAU Hospital, Jeddah, KSA) using the agar diffusion method as described formerly [25]. Briefly, 25 mL of inoculated Muller-Hinton agar petri dishes containing 1 mL, 1×10^6 CFU/mL of bacterial culture were prepared. Five holes, each 4 mm in diameter, were made in the plates. Twenty microliters of each sample at different concentrations (10, 20, and 40 mg/mL) were added, and water served as a negative control, while a standard antibiotic was a positive control, followed by incubation of the plates at 37 °C for 24 h. Antibacterial activity was recorded when no bacterial growth was observed around the holes. The zone of inhibition was recorded by a caliper.

Minimum inhibitory concentration

The antibacterial activity (concentrations ranging from 0.156 to 20 mg/mL) for each sample was also evaluated to determine the minimum inhibitory concentrations (MICs) according to the CLSI guidelines using the micro-broth dilution method [25]. Positive control ciprofloxacin was used. A loopful of bacterial cultures was added to 5 mL PBS, and turbidity was set to $1–5 \times 10^6$ CFU/mL. In 96 wells of tissue culture plates with 100 mL of Muller-Hinton broth per well and various concentrations of the samples, 10 µL of standardized bacterial culture were added. The MIC (µg/mL) was identified as the lowest concentration that prevents the bacterial strains from growing. All assays were performed in triplicate.

Antibiofilm assay

A qualitative assessment of the antibiofilm activity of BBG samples at 3 different concentrations (10, 20, and 40 mg/mL) was determined as previously described [25]. A loopful of bacterial cultures was added to tubes containing 5 mL Muller-Hinton broth and incubated at 37 °C for 24 h. The tubes were decanted and dried after being washed 3× with PBS (pH 7.3). Preserving the bacterial films was done by adding 5 mL of a 3.0%

sodium acetate solution for 15 min, followed by washing with water. Crystal violet (0.1% v/v) was used to stain the bacterial biofilms for 15 min, and then the excess dye was discarded and washed with de-ionized water. After that, tubes were dried inverted and checked for the development of biofilms. Positive biofilm formation was defined as the presence of a discernible coating on the tube's bottom and wall. Ring growth at the liquid interface was not considered a sign of the development of a biofilm. Following a thorough examination of the tubes, the amount of biofilm development was graded as 0-absent, 1-weak, 2-moderate, or 3-strong. The crystal violet dye was dissolved in 2 mL of ethanol. By using a UV-vis spectrophotometer set at 570 nm, the biofilms were measured. Using Eq. (2), the inhibition % was calculated;

$$\text{Inhibition } \% = \left(OD_c - \frac{OD_t}{OD_c} \right) \times 100 \quad (2)$$

where OD_c is the control's optical density (without glass), and OD_t is the optical density of the treatment.

■ RESULTS AND DISCUSSION

Results revealed that samples T1 and T3 showed the strongest biofilm inhibition activity with %inhibition 75.17 ± 2.61 and 65.77 ± 1.81, respectively. Accordingly, both T1 and T3 were further investigated.

XRD

The XRD configurations of the prepared glass systems (T1 and T3) are shown in Fig. 1. The XRD configurations of both samples show broad hump peaks rather than any crystalline peaks, indicating that the samples are of an amorphous structure [26].

XRF

The experimental compositions of the three borate glasses generated using the melt-quench process were found to be relatively close to the expected calculated composition, according to the XRF data shown in Table 2. The results suggested that the glass network structure was formed as intended. However, the high volatility of alkali-borate compounds during the melting process may be the reason for the small dissimilarities between theoretical and XRF findings [27]. The compositional changes between the theoretical and the experimental were

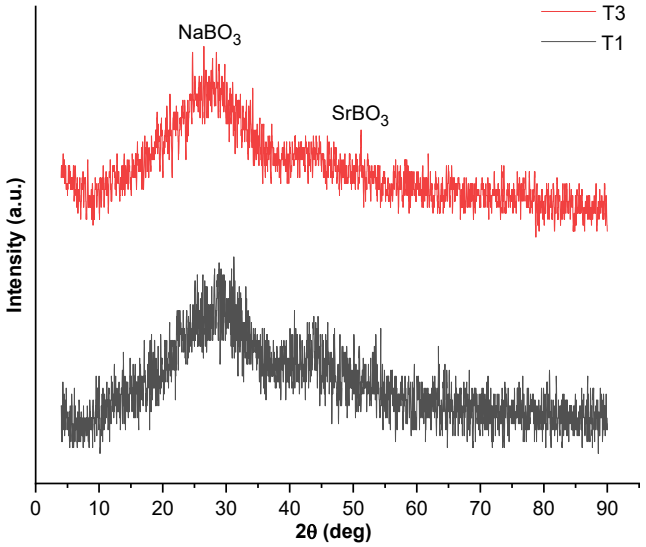

Fig 1. XRD pattern of the studied T1 and T3 strontium borate glasses

Table 2. Compositional analysis of the prepared BBG samples by XRF

Composition mol.% /Bioactive glass	B_2O_3	SrO	Li_2O	Na_2O	TiO_2	CaF_2
T1	51.11	25.03	16.92	5.18	0	1.76
T2	51.03	26.10	15.42	5.04	2.41	0
T3	50.29	25.37	14.13	5.14	5.07	0

negligibly minor and would barely affect the glass's bioactivity. Also, in the T3 sample, it was noticed that the measured CaF_2 level was a little lower than the calculated value. This may be attributed to the loss of some fluorine in the form of HF during the melting process [28].

FTIR Absorption Spectra

A method for examining the structure of both crystalline and non-crystalline materials is considered to be FTIR spectroscopy. It is also utilized to identify a material's numerous structural groups as well as any structural modifications made, such as composition alterations and irradiation processes [29].

Additionally, it defines the glass structure and explains how the various metal oxides are placed and interrelated with their neighboring ions in the glassy network [30]. The trigonal BO_3 units, which join to form the six-membered boroxol ring, and the tetrahedral BO_4 groups are the basic structural building blocks of the borate structure. The splitting of B–O–B bonds that

result from the hosting of network modifier oxides like alkali ions, transition metal ions, and rare earth ions results in the creation of more NBO, which in turn causes the transformation of triangular planar sp^2 BO_3 units into tetrahedral sp^3 BO_4 groups with penta-, tetra-, tri-, and di-borate groups. This method depends on the inserted ions' kind, concentration, and interactions with the other ions in the area.

The structure of alkali-metal borate glasses has been simultaneously revealed in three distinct boron positions: ring BO_3 units positioned within six-membered boroxol or borate rings, non-ring BO_3 units positioned outside the rings, and BO_4 units. BO_3 units that do not form a ring can be converted to BO_4 units by introducing alkali metal ions to boron oxide. Boroxol rings are transformed to six-membered rings with one BO_4^- tetrahedron such as triborate, tetraborate, pentaborate, or six-membered rings with two BO_4^- tetrahedral (diborate) by the addition of metal oxide to boron [30-31]. The addition of low percentages of 3d transition metal oxide, such as titanium oxide (TiO_2), is not expected to create noticeable modifications in the FTIR spectra of either the primary structural building components or their arrangements. Transition metal ions, when doped in low percentages, act as network modifiers.

Fig. 2 and 3 show the FTIR absorption spectra of the manufactured TiO_2 and CaF_2 strontium borate glasses before and after 40 kGy gamma irradiation, revealing certain common structural units in the three examined strontium borate structures. Herein, the interpretation of the communal indispensable structural groups in the three investigated glasses according to FTIR absorbance spectra. The characteristic tiny bands formed in the far-IR region centered at 428–462 cm^{-1} were attributed to the bending vibration of the inserted modifier ions, such as Li^+, Na^+, or Sr^{2+} ions, in their interstitial sites, including bridging and non-bridging kinds [32-33]. The presence of high concentrations of alkali ions (45%) in the glassy structure aids in occupying interstitial sites and boosting the synthesis of NBOs via nonlinear variations in borate network connectivity. This behavior allows the glass to melt at a relatively low temperature (850 °C), where alkali ions are known as "fluxes" [34]. The observed small broad bands at 510 and 590 cm^{-1} may be attributed to B–O–B bending vibrations, while the bending vibration of (B–O–B) triangular borate linkages was associated with an observed strong absorption band centered at 706 cm^{-1} [35]. The asymmetrical stretching vibration of B–O bonds in tetrahedral BO_4 units delivered high sharp bands in the 800–1,200 cm^{-1} area. TiO_2-doped glass has bands at 920 and 990 cm^{-1}, and CaF_2 has bands at 826, 890, and 955 cm^{-1} [36]. The bands at 1,200–1,600 cm^{-1} are related to stretching vibration of trigonal BO_3 units, such as bands at 1,210 and 1,390 cm^{-1} for TiO_2 doped glass

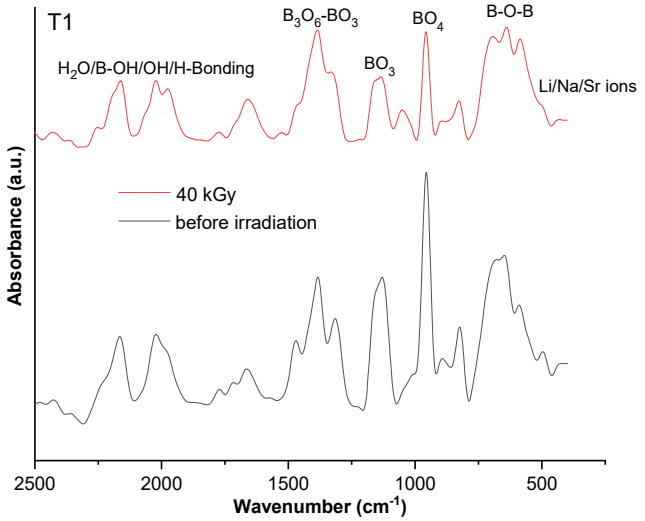

Fig 2. FTIR spectra measurements of T1 strontium borate glass before and after 40 kGy of gamma radiation

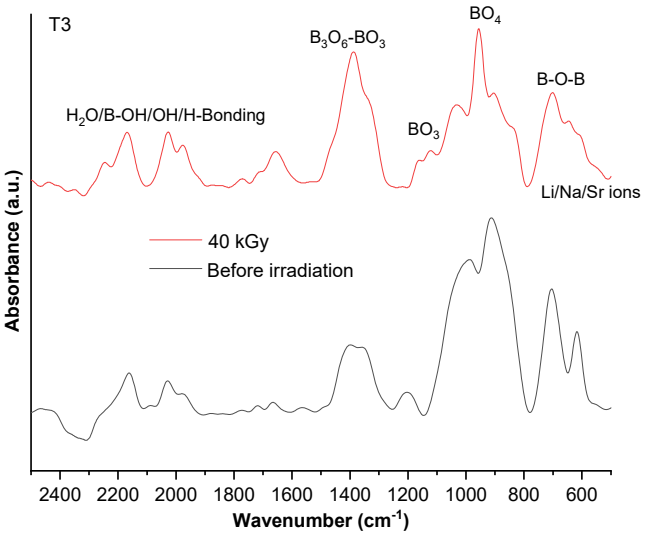

Fig 3. FTIR spectra measurements of T3 strontium borate glass before and after 40 kGy of gamma radiation

and bands at 1,320, 1,390, 1,470, and 1,670 cm^{-1} for CaF_2 doped glass. The high distinctive band, 1,390 cm^{-1} for the two glasses, can be correlated to diborate ring vibrations between B_3O_6-BO_3 links and/or stretching vibration of tetra/penta-borate rings [37]. Many observed bands were discovered in the region 1,600–4,000 cm^{-1} linked with the vibration of H-bonded, such as broad bands nearly at 2,000–2,300 cm^{-1}, in addition to the vibrations of molecular H_2O, OH, and B–OH units [38-39].

On the other hand, irradiating glasses with gamma rays (40 kGy) caused some modifications in the FTIR spectra, such as increasing band sharpness and shifting peaks to longer wavenumbers. As is well known, borate glasses have three or four coordinations, with the random borate network consisting primarily of trigonal BO_3 units connected by bridge oxygens (B–O–B). Ionizing radiation, such as X-rays, gamma rays, and/or electron beams, can cause certain dislocations and atomic displacements in glass, resulting in a more interrupted or disordered glass structure. As a result of the increase in NBO concentration, trigonal BO_3 is converted to tetrahedral BO_4, resulting in the development of various structural units such as di-, tri-, tetra-, or penta-borate. Irradiation also induces the creation of "Frenkel pairs," which causes the glass connection to rupture due to differences in bond angles and/or bond lengths of the main structural groups. As a result of the clear effect of gamma radiation on the examined glass structure, vibrational bands would move and sharpness would rise [26,29,40].

Density and Molar Volume

Glass density is an important physical measure used to investigate material tightness and structural changes [41]. It relates to the matching of masses and volumes; therefore, density is directly tied to the chemical composition of the host glass and how its atomic groups are associated with one another [41-42]. The addition of modifier oxide/ions changes the glass density values depending on the concentration of injected ions and how they interact with other glass components. As obvious in Fig. 4, the highest density was for 5% TiO_2, followed by 2% CaF_2, then the glass doped 2% TiO_2. Density can alternatively be defined as weight per unit volume. As a result, it is directly connected to the molar mass of the inserted metal ions, where CaF_2 and TiO_2 have a molar mass of 78.07, and 79.86 g/mol, respectively. Accordingly, the density values of the three glasses are relatively close and have the last order according to the weight or molar mass of the introduced ions and their concentrations. The observed increase in TiO_2 glass density could be attributed to the presence of Ti^{4+} ions in the glassy network in the form of compacted TiO_4 and TiO_6, which can affect charge balance and hinder the creation of new NBOs, resulting in more compacted and denser structures [43]. As demonstrated in Fig. 4 and Table 3, the irradiation procedure causes a minor drop in the density values and a slight increase in the molar volume values of the three examined glasses. This behavior is due to the effect of such ionizing radiation on the glass host structure, where atomic

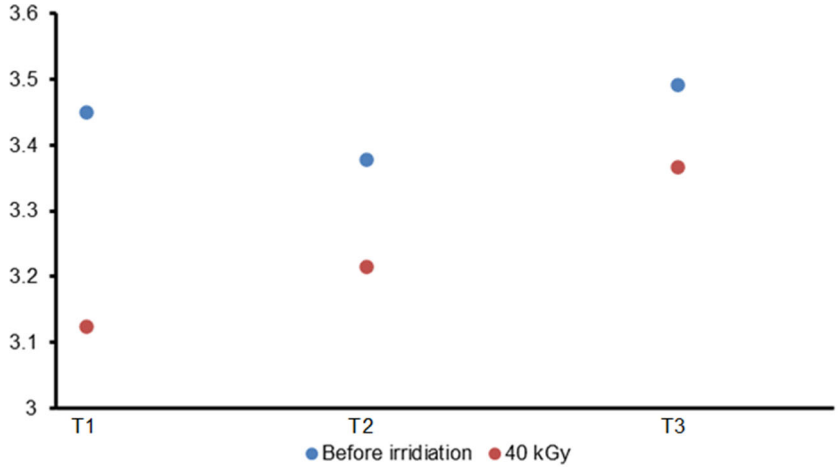

Fig 4. The density of the three examined glasses both before and after 40 kGy of gamma radiation

Table 3. Molar volume (V_m) values of the BBG samples

Glass samples	Glass composition						Molar mass (M) (g/mol)	Density (ρ) (g/cm³)		V_m before irradiation (cm³/mol)	V_m after irradiation (cm³/mol)
	B_2O_3	SrO	Li_2O	Na_2O	TiO_2	CaF_2		before irradiation	after irradiation		
T1	50	25	15	5	0	2	69.83	3.45	3.12	20.24	22.38
T2	50	28	15	5	2	0	72.97	3.38	3.22	21.59	22.66
T3	50	28	15	5	5	0	75.37	3.50	3.37	21.53	22.36

displacements and electronic flaws result in a decrease in the number of NBO atoms, which causes a decrease in density [39].

Antibacterial Bioassay

In an *in vitro* antibacterial bioassay, the three strontium borate samples were evaluated at three different concentrations (10, 20, and 40 mg/mL) by agar diffusion technique, followed by MIC determination at concentration ranges 0.156–20 mg/mL against a standard strain of *P. aeruginosa* and the results were listed in the shown Fig. S1 and S2. The samples studied possessed no antimicrobial activity toward the selected microorganism. Assessment of the formation of biofilm was done as described previously by Christensen et al. [44]. This was in accordance with the 2017 study by Farag et al. [45], which examined the antibacterial activity of two bioactive glasses, S5-0 and S5-25, against *Bacillus subtilis*, *Staphylococcus pneumonia*, *Escherichia coli*, and *P. aeruginosa*. The findings revealed that S5-0 glass had no inhibitory activity against *P. aeruginosa* but showed moderate inhibitory activity against *B. subtilis* (18.2 mm), *S. pneumonia* (17.1 mm), and *E. coli* (16.9 mm) [45].

Agar diffusion assays were used in a different study by Wilkinson et al. [46] to test silver Bioactive Glass (Bg^{Ag}) against planktonic cultures of *P. aeruginosa* and *S. aureus*, and the results showed that the two types of bioactive glass had different effects on the strains under study. Interestingly, BG had no inhibitory effect on *S. aureus* yet was modestly efficient at preventing *P. aeruginosa* growth. In contrast, following 24- or 48-h treatments, Bg^{Ag} induced substantial antimicrobial activity against both *P. aeruginosa* and *S. aureus* [46].

The amount of biofilm formation was graded as 0-absent, 1-weak, 2-moderate, or 3-strong, and the inhibition percentage was valued. A qualitative assessment of the antibiofilm activity of borate glass samples at 3 different concentrations, namely 10, 20, and 40 mg/mL, was determined using the tube method (Fig. 5, 6, S3, and S4). Results revealed that sample T1 showed strong biofilm inhibition activity with an inhibition percentage of 75.17 ± 2.61% (strong), followed by sample T3 with 65.77 ± 1.81% (moderate), then 54.37 ± 0.99% for T2 (weak) at the highest concentration studied. The release of fluoride ions may be the reason for the highest antibiofilm activity of T1 BBG [47-48], while the presence of TiO_2 in both T2 and T3 samples may be the reason for less release of ions as TiO_2 may contribute to the glassy network as a former oxide that causes less nonbridging oxygens [49]. Surprisingly, after exposure of borate glass samples to gamma irradiation, sample T1 showed a moderate biofilm inhibition

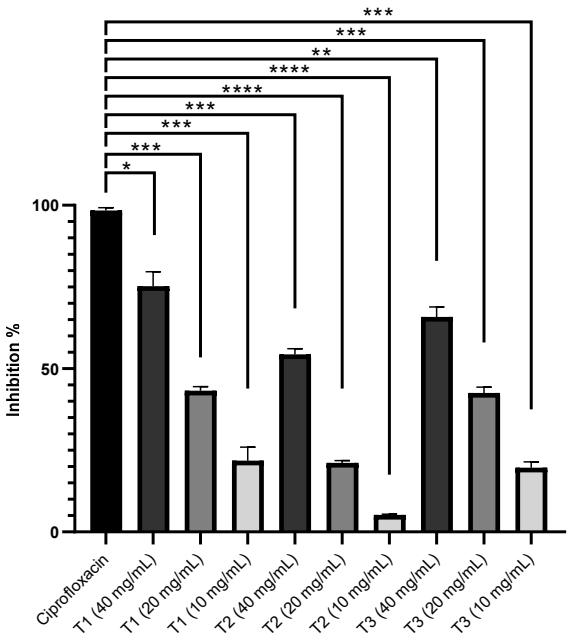

Fig 5. Biofilm inhibition percentage of borosilicate glass samples at three different concentrations against *P. aeruginosa*

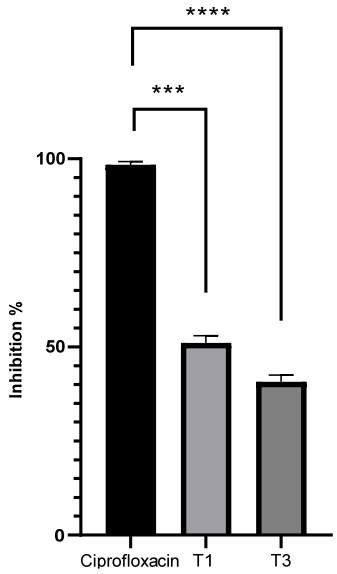

Fig 6. Biofilm inhibition percentage of T1 and T3 borate glass samples after radiation against *P. aeruginosa*

percentage of 51.3 ± 1.955% while sample T3 showed a weak biofilm inhibition percentage of 40.73 ± 1.79%. In the same study by Wilkinson et al. [46], 0.625% Bg^{Ag} completely suppressed *S. aureus* biofilm formation, while 0.625% Bg treatment had no effect on *S. aureus* biofilm formation. Both Bg and Bg^{Ag} significantly prevented biofilm development for *P. aeruginosa* at higher concentrations (0.625%). Only Bg^{Ag}, however, was able to partially prevent biofilm development at the lower 0.15%. These results show that Bg^{Ag} is more effective at preventing biofilms than Bg alone [46]. This work primarily presented gamma irradiation as a sterilizing procedure, an enhancement to bulk characteristics, and a surface modification of glass. Due to the formation of defects brought on by this irradiation, gamma irradiation is thought of as a modifier for the glass network. Although the irradiation process can be assumed to make some structural changes, including displacement, radiolysis, and/or electronic rearrangements. Thus, an increase in the glass surface area for a less antibiofilm effect, this may be due to an unexpected decrease in leaching of glass components. This weak effect may be attributed to this borate glasses' robust, compact structure, which contains multipurpose structural building blocks (BO_4, BO_3, TiO_4). By combining modifying cations to make up for the excess negative charges of BO_4 and TiO_4, which are firmly bound within the structure, this collective arrangement may decrease the nonbridging oxygens. Hence, the liberated ions are relatively few, and all the expected variations are quite low [45,49]. Therefore, the irradiation process could have a negative effect on antibiofilm glass activity. Accordingly, irradiation can't be recommended for sterilization and cannot be recommended for enhancing the antibiofilm effect against *P. aeruginosa.*

■ CONCLUSION

Three strontium borate glass compositions have been prepared and characterized. Trigonal BO_3 and tetrahedral BO_4 group vibrations were noted in the FTIR spectrum. Sharpness and shifting peaks to longer wavenumbers and molar volume and density changes were detected before and after 40 kGy gamma irradiation. Samples T1 and T3 displayed higher antibiofilm potential against *P. aeruginosa* than that of T2. Before irradiation, the presence of TiO_2 in T2 and T3 plays an important role in the decrease of NBOs and, thus, lower release of ions than T1, which also releases fluoride ions. On the other hand, the irradiation procedure had an unexpected detrimental effect on the glass antibiofilm activity, which could be attributed to structural alterations that resulted in a greater decrease in NBOs and, hence, ion liberation. As a result, irradiation is not suggested for improving the antibiotic efficacy of these BGs against *P. aeruginosa*. As a result, additional research should be conducted to assess the effect of these samples on other bacterial strains, as well as the potential combination of these created bioglasses with antibiotics against some antibiotic-resistant pathogens.

■ CONFLICT OF INTEREST

The authors declare that they have no known competing financial interests or personal relationships that could have appeared to influence the work reported in this paper.

■ AUTHOR CONTRIBUTIONS

Eman Mohamed Abou Hussein and Mahmoud Abdelkhalek Elfaky conducted the experiment, Noha

Mohamed Abou Hussien and Tamer Dawod Abdelaziz analyzed the data, Sabrin Ragab Mohamed Ibrahim, Mahmoud Abdelkhalek Elfaky, Eman Mohamed Abou Hussein, Tamer Dawod Abdelaziz wrote and revised the manuscript. All authors agreed to the final version of this manuscript.

■ REFERENCES

[1] Salehi, B., Abu-Darwish, M.S., Tarawneh, A.H., Cabral, C., Gadetskaya, A.V., Salgueiro, L., Hosseinabadi, T., Rajabi, S., Chanda, W., Sharifi-Rad, M., Mulaudzi, R.B., Ayatollahi, S.A., Kobarfard, F., Arserim-Uçar, D.K., Sharifi-Rad, J., Ata, A., Baghalpour, N., and Contreras, M.M., 2019, *Thymus* spp. plants - Food applications and phytopharmacy properties, *Trends Food Sci. Technol.*, 85, 287–306.

[2] Impey, R.E., Hawkins, D.A., Sutton, J.M., and Soares da Costa, T.P., 2020, Overcoming intrinsic and acquired resistance mechanisms associated with the cell wall of Gram-negative bacteria, *Antibiotics*, 9 (9), 623.

[3] Ibargüen-Mondragón, E., Romero-Leiton, J.P., Esteva, L., Cerón Gómez, M., and Hidalgo-Bonilla, S.P., 2019, Stability and periodic solutions for a model of bacterial resistance to antibiotics caused by mutations and plasmids, *Appl. Math. Modell.*, 76, 238–251.

[4] Matharu, R.K., Charani, Z., Ciric, L., Illangakoon, U.E., and Edirisinghe, M., 2018, Antimicrobial activity of tellurium-loaded polymeric fiber meshes, *J. Appl. Polym. Sci.*, 135 (25), 46368.

[5] Ottomeyer, M., Mohammadkah, A., Day, D., and Westenberg, D., 2016, Broad-spectrum antibacterial characteristics of four novel borate-based bioactive glasses, *Adv. Microbiol.*, 6 (10), 776–787.

[6] Zhou, P., Garcia, B.L., and Kotsakis, G.A., 2022, Comparison of antibacterial and antibiofilm activity of bioactive glass compounds S53P4 and 45S5, *BMC Microbiol.*, 22 (1), 212.

[7] Fernandes, J.S., Gentile, P., Pires, R.A., Reis, R.L., and Hatton, P.V., 2017, Multifunctional bioactive glass and glass-ceramic biomaterials with antibacterial properties for repair and regeneration of bone tissue, *Acta Biomater.*, 59, 2–11.

[8] Drago, L., Toscano, M., and Bottagisio, M., 2018, Recent evidence on bioactive glass antimicrobial and antibiofilm activity: A minireview, *Materials*, 11 (2), 326.

[9] El-Tablawy, S., Abd-Allah, W., and Araby, E., 2018, Efficacy of irradiated bioactive glass 45S5 on attenuation of microbial growth and eradication of biofilm from AISI 316 L discs: *In-vitro* study, *Silicon*, 10 (3), 931–942.

[10] El-Batal, H., El-Kheshen, A.A., El-Bassyouni, G.T., and Abd El Aty, A.A., 2018, *In vitro* bioactivity behavior of some borate glasses and their glass-ceramic derivatives containing Zn^{2+}, Ag^{+} or Cu^{2+} by immersion in phosphate solution and their anti-microbial activity, *Silicon*, 10 (3), 943–957.

[11] Moghanian, A., Ghorbanoghli, A., Kazem-Rostami, M., Pazhouheshgar, A., Salari, E., Saghafi Yazdi, M., Alimardani, T., Jahani, H., Sharifian Jazi, F., and Tahriri, M., 2020, Novel antibacterial Cu/Mg-substituted 58S-bioglass: Synthesis, characterization, and investigation of *in vitro* bioactivity, *Int. J. Appl. Glass Sci.*, 11 (4), 685–698.

[12] Valappil, S.P., and Higham, S.M., 2014, Antibacterial effect of gallium and silver on *Pseudomonas aeruginosa* treated with gallium–silver–phosphate-based glasses, *Bio-Med. Mater. Eng.*, 24 (3), 1589–1594.

[13] Esfahanizadeh, N., Nourani, M.R., Bahador, A., Akhondi, N., and Montazeri, M., 2018, The anti-biofilm activity of nanometric zinc doped bioactive glass against putative periodontal pathogens: An *in vitro* study, *Biomed. Glasses*, 4 (1), 95–107.

[14] Abou Neel, E.A., Hossain, K.M.Z., Abuelenain, D., Abuhaimed, T., Ahmed, I., Valappil, S.P., and Knowles, J.C., 2021, Antibacterial effect of titanium dioxide-doped phosphate glass microspheres filled total-etch dental adhesive on *S. mutans* biofilm, *Int. J. Adhes. Adhes.*, 108, 102886.

[15] Bari, A., Bloise, N., Fiorilli, S., Novajra, G., Vallet-Regí, M., Bruni, G., Torres-Pardo, A., González-Calbet, J.M., Visai, L., and Vitale-Brovarone, C., 2017, Copper-containing mesoporous bioactive

glass nanoparticles as multifunctional agent for bone regeneration, *Acta Biomater.*, 55, 493–504.

[16] Zhou, J., Wang, H., Zhao, S., Zhou, N., Li, L., Huang, W., Wang D., and Zhang, C., 2016, *In vivo* and *in vitro* studies of borate-based glass micro-fibers for dermal repairing, *Mater. Sci. Eng., C*, 60, 437–445.

[17] Maany, D.A., Alrashidy, Z.M., Abdel Ghany, N.A., and Abdel-Fattah, W.I., 2019, Comparative antibacterial study between bioactive glasses and vancomycin hydrochloride against *Staphylococcus aureus*, *Escherichia coli*, and *Pseudomonas aeruginosa*, *Egypt Pharm. J.*, 18 (4), 304–310.

[18] Han, T., Stone-Weiss, N., Huang, J., Goel, A., and Kumar, A., 2020, Machine learning as a tool to design glasses with controlled dissolution for healthcare applications, *Acta Biomater.*, 107, 286–298.

[19] Abd-Allah, W.M., and Fathy, R.M., 2022, Gamma irradiation effectuality on the antibacterial and bioactivity behavior of multicomponent borate glasses against methicillin-resistant *Staphylococcus aureus* (MRSA), *JBIC, J. Biol. Inorg. Chem.*, 27 (1), 155–173.

[20] Hall, C.W., and Mah, T.F., 2017, Molecular mechanisms of biofilm-based antibiotic resistance and tolerance in pathogenic bacteria, *FEMS Microbiol. Rev.*, 41 (3), 276–301.

[21] Ciofu, O., and Tolker-Nielsen, T., 2019, Tolerance and resistance of *Pseudomonas aeruginosa* biofilms to antimicrobial agents—How *P. aeruginosa* can escape antibiotics, *Front. Microbiol.*, 10, 913.

[22] İdil, Ö., Şahal, H., Canpolat, E., and Özkan, M., 2023, Synthesis, characterization, antimicrobial and time killing activities of new sulfa-derived Schiff bases coordinated with Cu(II), *Indones. J. Chem.*, 23 (3), 831–842.

[23] da Silva Aquino, K.A., 2012, "Sterilization by gamma irradiation" in *Gamma Radiation*, Eds. Adrovic, F., IntechOpen, Rijeka, Croatia, 172–202.

[24] Chanshetti, U.B., Shelke, V.A., Jadhav, S.M., Shankarwar, S.G., Chondhekar, T.K., Shankarwar, A.G., Sudarsan, V., and Jogad, M.S., 2011, Density and molar volume studies of phosphate glasses, *FU Phys. Chem. Technol.*, 9 (1), 29–36.

[25] Clinical Laboratory Standard Institute, 2006, *Zone diameter Interpretive Standards and corresponding minimal inhibitory concentration (MIC) interpretive break point, Supplement M44-S1*, Clinical and Laboratory Standard Institute, Wayne, PA.

[26] Madhu, A., Eraiah, B., and Srinatha, N., 2020, Gamma irradiation effects on the structural, thermal, and optical properties of samarium doped lanthanum–lead-boro-tellurite glasses, *J. Lumin.*, 221, 117080.

[27] Fernandes, J.S., Gentile, P., Moorehead, R., Crawford, A., Miller, C.A., Pires, R.A., Hatton, P.V., and Reis, R.L., 2016, Design and properties of novel substituted borosilicate bioactive glasses and their glass-ceramic derivatives, *Cryst. Growth Des.*, 16 (7), 3731–3740.

[28] Swansbury, L.A., 2017, A Structural Investigation of Chlorine-Containing and Fluorine-Containing Oxide Glasses Using Molecular Dynamics, Neutron Diffraction, and X-ray Absorption Spectroscopy *Dissertation*, University of Kent, UK.

[29] Almuqrin, A.H., Kumar, A., Prabhu, N.S., Jecong, J.F.M., Kamath, S.D., and Abu Al-Sayyed, M.I., 2022, Mechanical and gamma-ray shielding examinations of Bi_2O_3–PbO–CdO–B_2O_3 glass system, *Open Chem.*, 20 (1), 808–815.

[30] Abou Hussein, E.M., Madbouly, A.M., Ezz Eldin, F.M., and ElAlaily. N.A., 2021, Evaluation of physical and radiation shielding properties of Bi_2O_3–B_2O_3 glass doped transition metals ions, *Mater. Chem. Phys.*, 261, 124212.

[31] Abou Hussein, E.M., 2019, Characterization of some chemical and physical properties of lithium borate glasses doped with CuO and/or TeO_2, *J. Chem. Soc. Pak.*, 41, 52–61.

[32] Mohan, S., Kaur, S., Singh, D.P., and Kaur, P., 2017, Structural and luminescence properties of samarium doped lead alumino borate glasses, *Opt. Mater.*, 73, 223–233.

[33] Abou Hussein, E.M., El-Agawany, F.I., and Rammah, Y.S., 2022, CuO reinforced lithium-borate glasses: Fabrication, structure, physical properties, and ionizing radiation shielding competence, *J. Aust. Ceram. Soc.*, 58 (1), 157–169.

[34] Abou Hussein, E.M., 2019, Vitrified municipal waste for the immobilization of radioactive waste: Preparation and characterization of borosilicate glasses modified with metal oxides, *Silicon*, 11 (6), 2675–2688.

[35] Abou Hussein, E.M., and Barakat, M.A.Y., 2022, Structural, physical and ultrasonic studies on bismuth borate glasses modified with Fe_2O_3 as promising radiation shielding materials, *Mater. Chem. Phys.*, 290, 126606.

[36] El Batal, H.A., Abou Hussein, E.M., El Alaily, N.A., and EzzEldin, F.M., 2020, Effect of different 3d transition metal oxides on some physical properties of γ-Irradiated Bi_2O_3- B_2O_3 glasses: A comparative study, *J. Non-Cryst. Solids*, 528, 119733.

[37] Ahmad, Z., Ali, S., Ahmad, H., Hayat, K., Iqbal, Y., Zulfiqar, S., Zaman, F., Rooh, G., and Kaewkhao, J., 2020, Radio-optical response of cerium-doped lithium gadolinium bismuth borate glasses, *J. Lumin.*, 224, 117341.

[38] Abd El-Rehim, A.F., Shaaban, K.S., Zahran, H.Y., Yahia, I.S., Ali, A.M., Abou Halaka, M.M., Makhlouf, S.A., Abdel Wahab, E.A., and Shaaban, E.R., 2021, Structural and mechanical properties of lithium bismuth borate glasses containing molybdenum (LBBM) together with their glass–ceramics, *J. Inorg. Organomet. Polym. Mater.*, 31 (3), 1057–1065.

[39] Halimah, M.K., Chiew, W.H., Sidek, H.A.A., Daud, W.M., Wahab, Z.A., Khamirul, A.M., and Iskandar, S.M., 2014, Optical properties of lithium borate glass $(Li_2O)_x(B_2O_3)$, *Sains Malays.*, 43 (6), 899–902.

[40] Abou Hussein, E.M., 2023, The impact of electron beam irradiation on some novel borate glasses doped V_2O_5; Optical, physical and spectral investigation, *Inorg. Chem. Commun.*, 147, 110232.

[41] El-Alaily, N.A., Abou Hussein, E.M., and Ezz Eldin, F.M., 2018, Gamma irradiation and heat treatment effects on barium borosilicate glasses doped titanium oxide, *J. Inorg. Organomet. Polym. Mater.*, 28, 2662–2676.

[42] Bhogi, A., Vijaya Kumar, R., and Kistaiah, P., 2015, Effect of alkaline earths on spectroscopic and structural properties of Cu^{2+} ions-doped lithium borate glasses, *J. Non-Cryst. Solids*, 426, 47–54.

[43] Paramesh, G., and Varma, K.B.R., 2013, Structure-property correlation in BaO-TiO_2-B_2O_3 glasses: Glass stability, optical, hydrophobic, and dielectric properties, *Int. J. Appl. Glass Sci.*, 4 (3), 248–255.

[44] Christensen, G.D., Simpson, W.A., Bisno, A.L., and Beachey, E.H., 1982, Adherence of slime-producing strains of *Staphylococcus epidermidis* to smooth surfaces, *Infect. Immun.*, 37 (1), 318–326.

[45] Farag, M.M., Abd-Allah, W.M., and Ahmed, H.Y.A., 2017, Study of the dual effect of gamma irradiation and strontium substitution on bioactivity, cytotoxicity, and antimicrobial properties of 45S5 bioglass, *J. Biomed. Mater. Res., Part A*, 105 (6), 1646–1655.

[46] Wilkinson, H.N., Iveson, S., Catherall, P., and Hardman. M.J., 2018, A novel silver bioactive glass elicits antimicrobial efficacy against *Pseudomonas aeruginosa* and *Staphylococcus aureus* in an *ex vivo* skin wound biofilm model, *Front. Microbiol.,* 9, 1450.

[47] Fayad, A.M., Fathi, A.M., El-Beih, A.A., Taha, M.A., and Abdel-Hameed, S.A.M., 2019, Correlation between antimicrobial activity and bioactivity of Na-mica and Na-mica/fluorapatite glass and glass-ceramics and their corrosion protection of titanium in simulated body fluid, *J. Mater. Eng. Perform.*, 28 (9), 5661–5673.

[48] Abdelghany, A.M., and Kamal, H., 2014, Spectroscopic investigation of synergetic bioactivity behavior of some ternary borate glasses containing fluoride anions, *Ceram. Int.*, 40 (6), 8003–8011.

[49] Elbatal, H.A., Azooz, M.A., Saad, E.A., EzzELDin, F.M., and Amin, M.S., 2018, Corrosion behavior mechanism of borosilicate glasses towards different leaching solutions evaluated by the grain method and FTIR spectral analysis before and after gamma irradiation, *Silicon*, 10 (3), 1139–1149.